

Applications and Measurements of Polycapillary X-Ray Optics¹

C. A. MACDONALD

Center for X-Ray Optics, University at Albany, Albany, New York 12222

Received December 22, 1993; revised August 15, 1994

The recent invention of Kumakhov polycapillary x-ray and neutron optics has expanded the ways x-ray beams can be controlled. X rays incident on the interior of glass tubes at small angles can be guided down the tubes by total external reflection. Now, arrays of curved tapered capillaries can be used to focus, collimate, and filter x-ray radiation. Extensive research is being conducted on the performance and potential applications of these optics. Potential medical applications include mammography, digital energy subtraction angiography, and focused beam therapy. Other applications are x-ray lithography, x-ray astronomy, crystal diffraction, x-ray fluorescence, and neutron prompt gamma analysis.

© 1996 Academic Press, Inc.

1. INTRODUCTION

1.1. Description

Kumakhov capillary optics, consisting of arrays of hollow glass tubes, is a new technology for controlling x-ray beams. X rays incident on the interior of the glass tubes at small angles are guided down the tubes by total external reflection. The idea of using total external reflection to control x rays is quite old (1) and is the basis of the grazing incidence mirrors commonly used in x-ray telescopes and synchrotron beam lines. However, these mirrors are limited in their application by an extremely small angular acceptance. Alternative optics, based on interference or diffraction, using single crystals, multilayers, and zone and phase plates are spectrally selective.

The use of total external reflection to guide x rays in single hollow glass tubes has been established for some time (2). This is used to produce beams of extremely small diameter. Recently the use of arrays of large numbers of curved glass polycapillaries to collect and steer x rays was introduced by Kumakhov and his collaborators (3). Multifiber optics are manufactured by inserting polycapillary fibers through metal grids, as shown in Fig. 1. A monolithic construction with no grids is shown in Fig. 2.

¹ This invited paper was presented at the "Monochromatic X-Ray Workshop" conference held in Nashville, Tennessee, October 29-30, 1993.

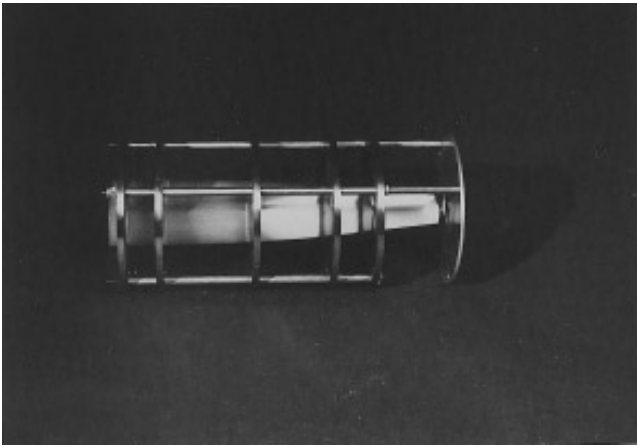


FIG. 1. Complete optic constructed from individual fibers strung through a metal grid.

1.2. Theory

The critical angle for total external reflection of x rays is approximately (4)

$$\theta_c \cong \frac{\omega_p}{\omega}, \quad (1)$$

where ω_p is the plasma frequency of the material. The plasma frequency is given by

$$\omega_p = \frac{Nq^2}{m\epsilon_0}, \quad (2)$$

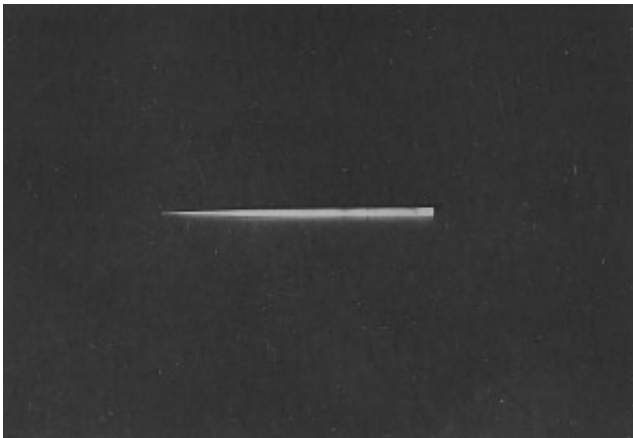


FIG. 2. Complete monolithic optic.

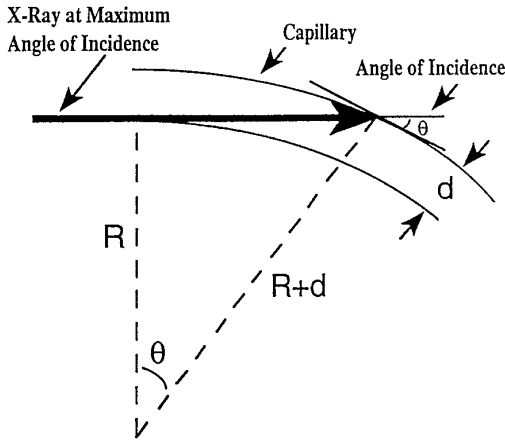


FIG. 3. Guiding of x-rays in bent channels. Figure adapted from Ref. (6).

where N is the electron density of the material, q and m are the electron charge and mass, respectively, and ϵ_0 is the vacuum dielectric constant. The critical angle is about 3 milliradians for 10 keV photons in glass, and is inversely proportional to the x-ray energy.

The x rays can be transmitted in a curved tube as long as the tube is small enough and bent gently enough that the angles of incidence are kept less than the critical angle. The maximum angle of incidence, as shown in Fig. 3, is given by

$$(R + d)\cos(\theta) = R, \quad (3)$$

where R is the bending radius of the fiber and d is the fiber diameter. Thus, by dividing by $(R + d)$ and using small quantity approximations,

$$\left(1 - \frac{\theta^2}{2}\right) \approx \frac{R}{R + d} = \frac{1}{1 + d/R} \approx 1 - \frac{d}{R}. \quad (4)$$

So the angle of incidence, which must be less than the critical angle, is

$$\theta^2 \approx \frac{2d}{R} < \theta_c^2. \quad (5)$$

For a given radius of curvature, this requires increasingly small diameter tubes as the x-ray energy is raised. In order to avoid the mechanical limitations of such small tube sizes, polycapillary fibers are employed with channel sizes (typically 5–30 μm) much

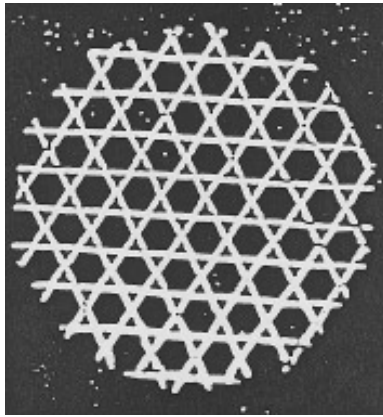


FIG. 4. Cross section of a borosilicate polycapillary. The channel size is about $17\ \mu\text{m}$.

smaller than the outer diameter ($300\text{--}1000\ \mu\text{m}$). A typical polycapillary fiber is shown in Fig. 4.

1.3. Transmission Measurements

Extensive measurements have been performed of transmission and exit divergence as a function of length, bend radius, x-ray source position, x-ray source geometry, and x-ray energy (5, 6). The measurements were performed for a variety of polycapillary compositions, diameters, and geometries. Transmission as a function of energy for two different polycapillary fiber types is shown in Fig. 5. Measured transmissions are as high as 78% at 15 keV and better than 50% from 1 to 44 keV. Preliminary measurements have demonstrated transmission through bent polycapillaries up to 150 keV (7).

Transmission falls exponentially with capillary length. The decay length varies with the manufacturing technique. Current technology capillaries yield a decay length of about 150 cm (5). Measurement technology has also improved. Using a computer automated test station, transmission measurements can be made to better than 1% accuracy (8).

1.4. Numerical Simulations

To evaluate the experimental performance of capillaries, design capillary optics, and evaluate potential applications, it is necessary to be able to predict theoretical behavior for complex geometries. To accomplish this goal, computer codes were developed based on Monte Carlo simulations of geometrical optics trajectories. The computational speed is greatly enhanced by a reduction to two dimensions by projecting the trajectory onto the local fiber cross section (9). Reflectivities are computed from standard tables (10). Roughness of the capillary walls can be taken into account

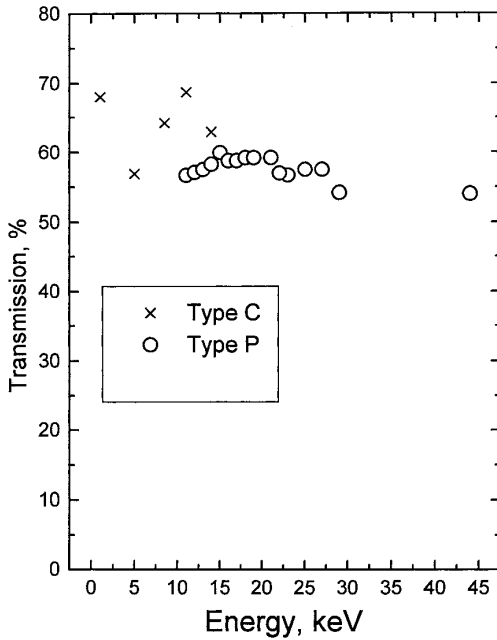


FIG. 5. Transmission as a function of energy for 12 cm long borosilicate polycapillaries from two different manufacturers. Type C have $17 \mu\text{m}$ channels, type P have $5 \mu\text{m}$ channels. Figure adapted from Ref. (5).

(11). However, in most cases for good quality fibers the simulations fit the data quite well without introducing roughness effects, that is, without any adjustable parameters.

2. COLLIMATING

Arrays of polycapillaries can be used to collect broadband divergent radiation and redirect it into a quasiparallel beam, as sketched in Fig. 6. The optic of Fig. 2 was designed for collimation.

For most applications of collimated beams, the divergence is an important parameter. The exit divergence from capillary optics is typically measured by rotating a high quality crystal in the beam and measuring the angular width of a Bragg peak. Because the exit divergence from the optics is much larger than the inherent Darwin width of the crystal or the width of the characteristic x-ray line, the measurement yields the divergence directly. The result for a single polycapillary is shown in Fig. 7. The full width at half maximum of the divergence from a polycapillary is typically about equal to the critical angle. A simple geometrical argument would yield a full width of twice the critical angle. However, because the reflectivity near the critical angle is less than the reflectivity at grazing incidence, large angle photons are preferentially lost in a long fiber. Measured exit divergence from a bent fiber is less than from a straight fiber due to the increased number of reflections.

The measured exit divergence from a multifiber lens is shown in Fig. 8. The

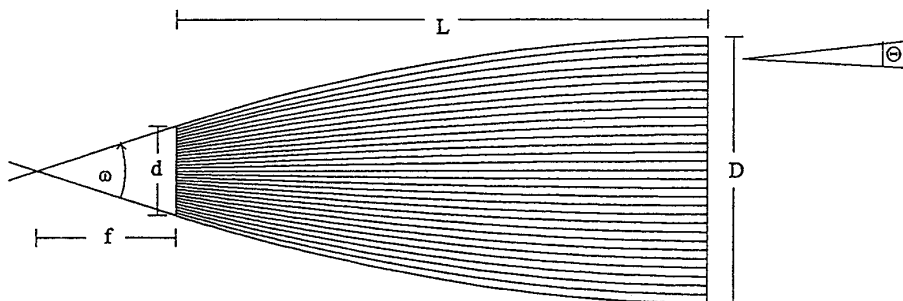


FIG. 6. Configuration of capillaries to collect and collimate radiation from a point source. Figure adapted from Ref. (14).

divergence has two components: the divergence of the individual polycapillaries and the fiber-to-fiber misalignment.

2.1. Diffraction

Preliminary measurements in a crystal diffraction experiment show that a flux gain of a factor of four to five is obtained by employing a multifiber optic compared to the optimized no optic condition for either a small sample single crystal diffraction experiment with pinhole collimation (12), or a double crystal diffraction experiment with slit collimation (13). Preliminary measurements on the newest generation of multifiber optics predict a substantially higher gain.

For very small samples, for example for protein crystallography, the more compact monolithic lens construction is required. Because of the large increase in collected solid angle compared to pinhole collimation, substantial gain is obtained even with

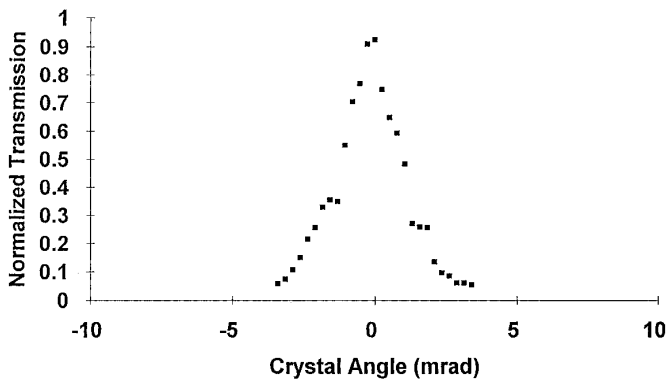


FIG. 7. Exit divergence from a 22 cm long bent polycapillary with $17 \mu\text{m}$ channels, measured using silver $K_{\beta 2}$ radiation and a germanium 111 reflection. The exit end has been displaced 1 mm. Figure adapted from Ref. (22).

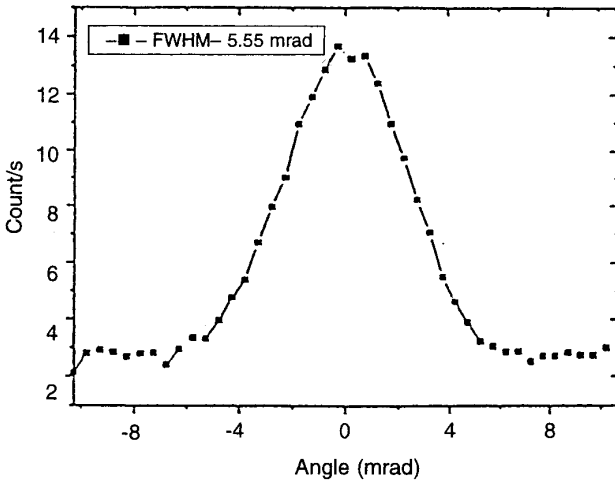


FIG. 8. Measured overall exit divergence from a multifiber polycapillary lens. Figure adapted from Ref. (5).

relatively poor transmission. Measurements of transmission and divergence of current monolithic prototypes yield an expected increase of intensity of about a factor of 35 into the desired angular width compared to pinhole collimation (14). True optimization with such a lens requires an intense microfocus source.

2.2. Lithography

It would be desirable to perform x-ray lithography for reduced feature sizes on high density integrated circuits without the need for a synchrotron facility. Aside from the considerable expense, a synchrotron could not be integrated into an existing production line. However, point sources of x rays would require collimation. Slit collimation results in too much loss of intensity for the required throughput. Capillary optics may provide a solution. Simulated field intensity for an optic designed for lithography (15) is shown in Fig. 9. The simulation is based on measurements of transmission and divergence performed at 1 keV.

Divergence requirements for lithography distinguish between the local divergence, labeled β in Fig. 10, and the overall angle subtended by the beam, α . In lithography, too large a local divergence results in a loss of resolution. Too small a divergence may result in unacceptable diffraction “ringing.” Similarly, too large a beam angle α causes unacceptable feature shift due to variations in the mask-to-wafer gap distance. However, a finite angle α is desired to allow for magnification adjustment by deliberately varying the gap. Acceptable values of the divergence are expected to be obtainable with multifiber capillary optics.

3. FOCUSING

Fewer Kumakhov lenses have been manufactured for focusing than for collimation. However, there are several intriguing potential applications.

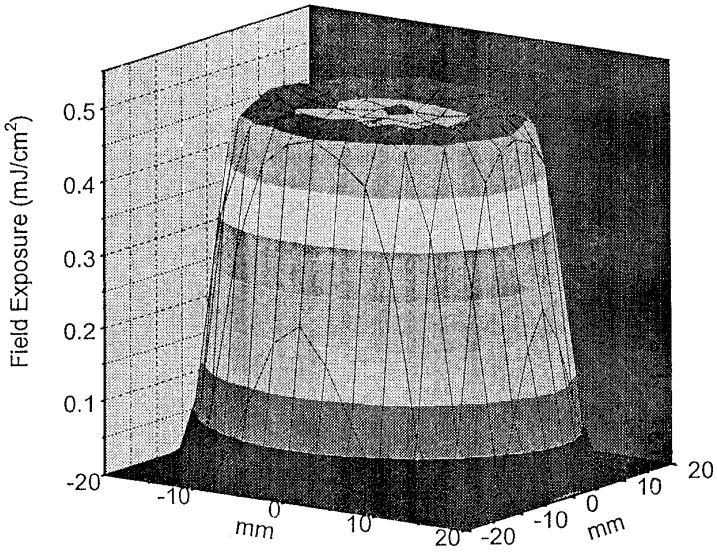


FIG. 9. Simulated field intensity for a multifiber polycapillary optic designed for microlithography. Figure adapted from Ref. (15).

18

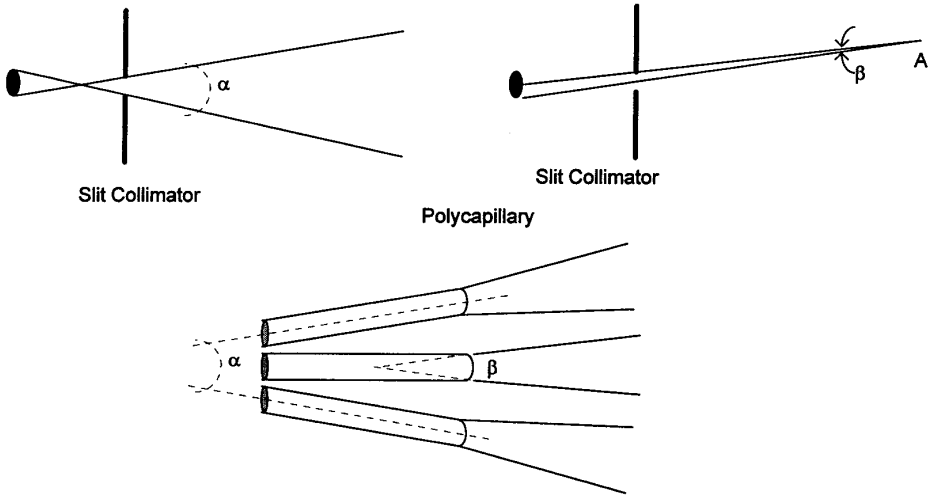


FIG. 10. For either a slit collimator or a polycapillary optic, the local divergence, β , seen at a point A is different than the angle subtended by the beam, α .

3.1. Focusing of Parallel Beams

3.1.1. Synchrotron. A capillary optic with a geometry similar to that designed to collimate a divergent beam could be used in reverse to focus a parallel input beam, such as a synchrotron beam, to produce extremely high fluxes. The geometry for focusing is not actually the reverse of that for collimation since sudden decreases in curvature are not harmful to transmission, but sudden increases are. Prototype monolithic optics with 6 mm entrance diameters, such as that shown in Fig. 2, have measured focal spot sizes of less than $100\ \mu\text{m}$ (16). This yields a flux gain of 3600τ , where τ is the transmission. A typical, rather imperfect, prototype has a measured transmission of 3% when used to collimate radiation from a point source. Used in reverse to focus parallel radiation, it is expected to have a transmission of about 0.2%. This yields an expected gain of about seven, even with this prototype. The poor transmission is a result of poor profile control. The measured transmission of the prototype agrees well with the simulation given the measured profile. However, an ideal profile has a simulated transmission an order of magnitude higher, even with the same channel size. Improvements in manufacturing techniques are expected to improve profile control. Decreasing the channel size would also improve the transmission. Numerical simulations yield intensity gains of a factor of 1000 for an ideal optic designed with $15\ \mu\text{m}$ channels for use at 8 keV.

Synchrotron applications would require good resistance to radiation damage. Polycapillaries appear to be relatively robust with respect to thermal damage because the thin walls preclude development of large thermal gradients. Preliminary measurements indicate that polycapillaries show only a slight, recoverable decrease in transmission at exposures of $700\ \text{kJ}/\text{cm}^2$.

3.1.2. Astronomy. Another source of parallel x-ray radiation is distant stars. Capillary optics could provide an efficient broadband collector for spectral analysis. Capillary optics are also extremely light in weight and inherently rigid from the honeycomb-like structure. Both properties are attractive since x-ray astronomy cannot be performed from an earth-based platform due to the strong absorption of the earth's atmosphere.

3.2. Focusing from a Point Source

Arrays of polycapillaries could also be used to collect broadband divergent radiation and redirect it towards a focal spot. The solid angle from which x rays can be captured, the capillary channel size, the x-ray energy, and the required length of the lens are related by the bending requirements of Eq. (5). The first Kumakhov capillary lens was built to demonstrate focusing and employed channel sizes of $300\ \mu\text{m}$ and was about 1 m in length (3, 17). Smaller channel sizes allow for tighter bending and shorter lenses. Transmission as a function of angular deflection at 8 keV is shown in Fig. 11 for a polycapillary with $17\ \mu\text{m}$ channels bent in a circular arc. Transmission for a similar polycapillary at 20 keV is shown (18) in Fig. 12. Beam deflections of 20 times the critical angle (4.7° at 8 keV) can be achieved with a transmission which is 70% of the straight fiber value.

3.2.1. Medical therapy. Conventional x-ray radiation therapy is currently performed with high energy x-ray radiation. The patient is exposed to multiple parallel beams

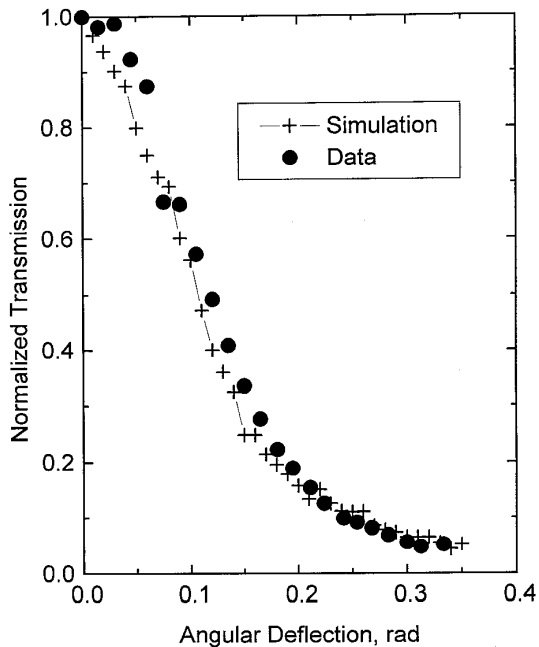


FIG. 11. Transmission at 8 keV as a function of beam deflection angle, for a 20 cm long polycapillary with $17 \mu\text{m}$ channel size bent in a circular arc. Values are relative to the straight fiber transmission. Solid line is simulation. Data are from Ref. (6).

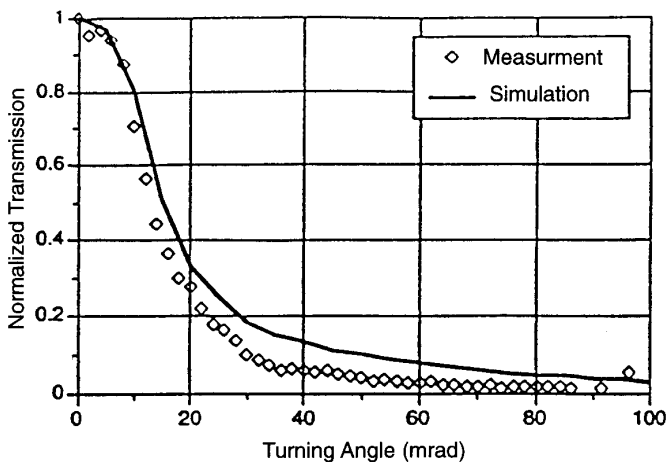


FIG. 12. Relative transmission at 20 keV as a function of deflection angle for a 22 cm long polycapillary with $17 \mu\text{m}$ channel size, bent by deflecting one end with the other held fixed (cubic one-point bending). Solid line is simulation. Figure adapted from Ref. (18).

with an intersection at the tumor. The parallel beams are produced with slit collimators. Gamma radiation is generally chosen to minimize the absorbed skin dose relative to the dose at the tumor, although energies as low as 150 keV are employed in the orthovoltage modality. Use of focusing capillary optics at energies around 100 keV could potentially substantially increase the tumor dose without increasing skin dose.

3.2.2. *X-ray photoelectron spectroscopy (XPS)*. The minimum focal spot achievable with a multifiber optic such as that shown in Fig. 1 is limited by the diameter of the polycapillary fiber used in its construction. This diameter is constrained by mechanical limitations to be larger than about 300 μm . The focal spot can be no smaller than that diameter since all of the channels in the fiber are parallel, not individually aimed at a single point. To achieve smaller focal spots, as would be required for materials microanalysis techniques such as XPS, it is necessary to taper the individual channels. This geometry requires the monolithic construction shown in Fig. 2. Focusing the radiation would provide significant signal gain over slit collimation.

3.2.3. *Fluorescence*. Focused x-ray beams would provide a similar benefit for microfluorescence analysis. The simulated intensity gain of the stimulating radiation from a monolithic optic compared to slit collimation is shown in Fig. 13. In addition, a second optic could be used to collect the fluorescent radiation (19). This would provide the double benefit of enhanced signal intensity and also three-dimensional spatial resolution. The three-dimensional resolution arises from the overlap of the cone of irradiation of the first lens and the cone of collection of the second, as shown in Fig. 14.

4. IMAGING

4.1. *Magnification and Demagnification*

Although capillary optics are not true imaging optics in the full theoretical sense, images can be transported in the optics in the same manner as in a coherent optical fiber bundle. By changing the diameter of the monolithic bundle, images can be magnified or demagnified (20). This could be useful for low resolution x-ray microscopy. It could also be employed to match the image size to the detector size, for example to demagnify a radiographic image to interface with a CCD detector. Alternatively, an image such as a mammogram could be magnified to be recorded on a detector which would otherwise not have sufficient resolution. While magnification by increasing the air gap in mammography results in a loss of resolution due to the geometrical blurring from the finite source size, magnification by capillary optics would not be subject to a loss of resolution. Magnification by a factor of 1.8 of a mammographic resolution test pattern has been demonstrated at 20 keV with a subsequent gain in resolution on a phosphor plate (21).

4.2. *Scatter Rejection*

Another potential application of the optic is scatter rejection for radiographic imaging. In mammography, for example, approximately half of the photons emerging

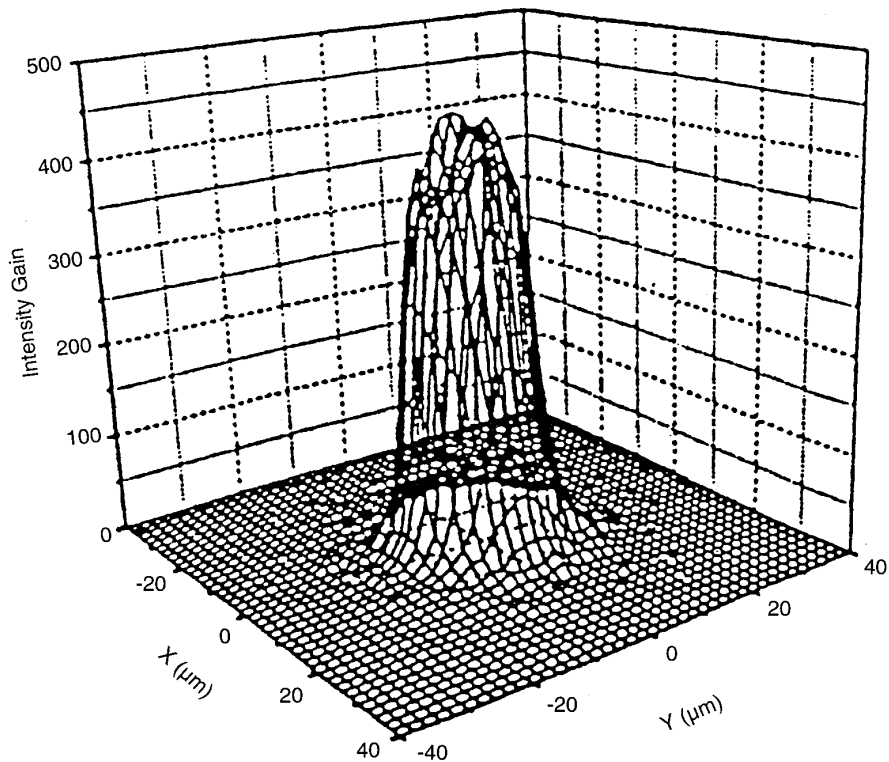


FIG. 13. Numerical simulation of intensity gain from a monolithic optic. Figure adapted from Ref. (5).

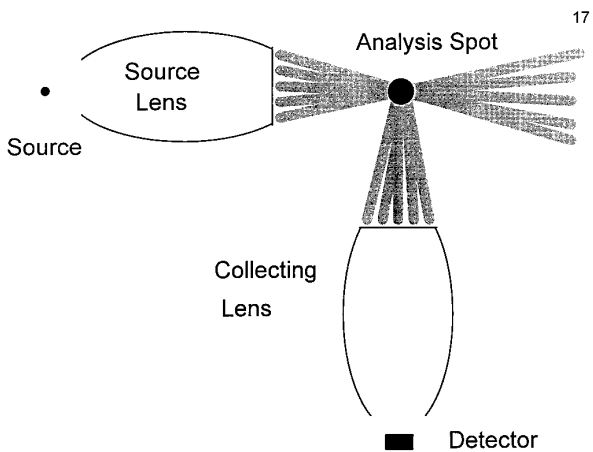


FIG. 14. Sketch of microfluorescence experiment, showing that overlap of irradiation and collection volumes yields three-dimensional spatial resolution.

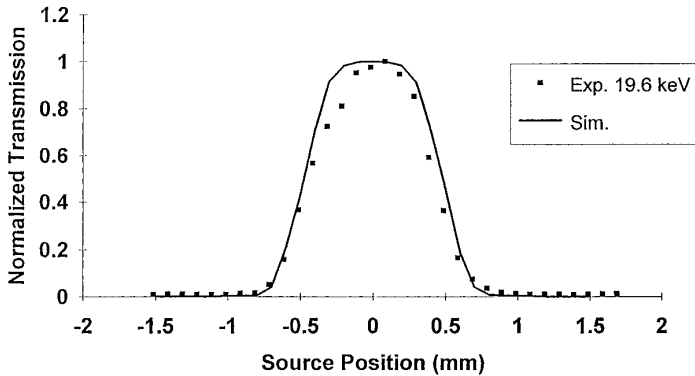


FIG. 15. Measured transmission, relative to the aligned value, as a function of lateral source displacement for a 22 cm long polycapillary with $17\ \mu\text{m}$ channels of 20 keV with a 30 cm source-to-fiber distance. Solid line is simulation. Figure adapted from Ref. (22).

from the breast have been scattered from their original trajectories. These photons degrade the subject contrast if not removed from the image. A conventional scatter rejection grid consists of lead strips separated by low density spacers. The thickness of the grid is a compromise between providing good transmission of the primary unscattered beam and low transmission of the scattered rays. A capillary optic could act as a nearly ideal scatter rejection grid, providing good primary transmission with nearly zero scatter transmission.

The good scatter rejection in the capillary optics arises from the low angular acceptance of each capillary channel. If a ray arrives at an angle greater than the critical angle it is not transmitted. The drop in transmission of a polycapillary as a function of source angle is shown (22) in Fig. 15. The source angle is increased by displacement of the source away from the fiber axis. Preliminary measurements with a bulk monolithic optic at the 20 keV energy typically used for mammography indicate that the photons which are not transmitted are effectively absorbed even in borosilicate glass. Measured scatter transmissions on small prototypes are less than 1% (22). An image produced by scanning a small prototype optic shows a nearly ideal contrast enhancement compared to a conventional grid (21).

5. ENERGY FILTRATION

The reflectivity of a glass surface as a function of energy and angle is shown in Fig. 16. The reflectivity at a particular angle can vary sharply with energy (e.g., the reflectivity drops rapidly between 6 and 8 keV at 5 mrad). Consider a fiber bent in the manner of Fig. 3 such that a large fraction of the beam is incident at angles greater than 5 mrad. The fiber will have a good transmission for energies less than 6 keV, but a low transmission for higher energies. In this manner, capillary optics can be designed which act as a low pass filter. This is a useful addition to absorption filters, which act as high pass filters.

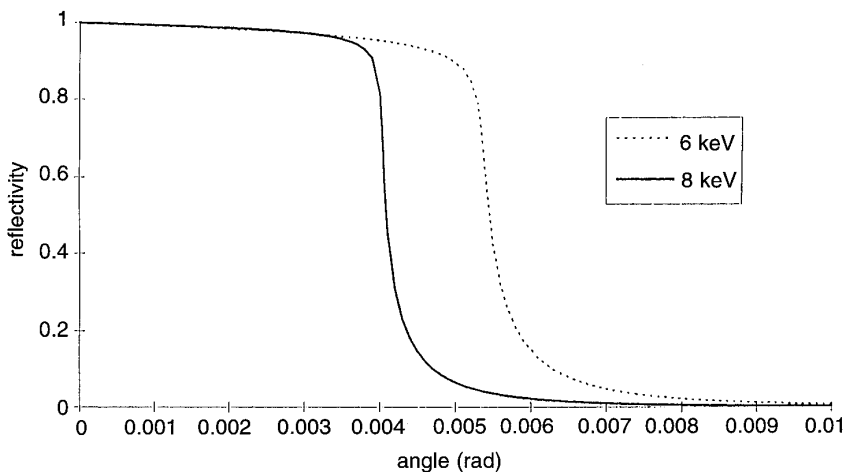


FIG. 16. Calculated reflectivity as a function of the angle between the incident beam and the glass surface for 6 keV (dotted line) and 8 keV (solid line). The critical angles are 5.5 and 4 mrad, respectively. Figure adapted from Ref. (6).

A capillary optics low pass filter could be used to remove high energy bremsstrahlung photons from a source in which a high anode voltage has been used to increase the intensity of the characteristic lines. An application which is being investigated is a rotating anode Ba/Ce source for digital energy subtraction angiography (23). The energy of the Ba $K\alpha$ emission is below the absorption edge for the iodine contrast agent injected into the patient. The Ce $K\alpha$ emission is at an energy above the edge. The received signal from the Ba emission is due to the bulk of the bone and tissue. The signal from the Ce emission is due to the bulk plus the iodine in the vascular system. The difference between the signals is predominately due to the vascular system. Digital energy subtraction angiography has been performed at a synchrotron because of the need for high intensity beams with narrow energy bandwidth. In order to design a source which would obviate the need for a synchrotron, the anode voltage was increased to 600 kVp to produce the requisite intensity. However, the high energy bremsstrahlung photons would increase the dose to the patient while reducing the subject contrast. These photons could be removed by a capillary optic filter.

6. NEUTRONS

The response of a material to a neutron can be written in a manner analogous to the response to a photon. The neutron index of refraction for most materials has a real part which is slightly less than one for low energy neutrons. The critical angles for thermal and colder neutrons are similar to the critical angles for x rays in the vicinity of 10 keV. Transmission and focusing of neutrons have been demonstrated with polycapillary optics (24). Applications which are being investigated include prompt gamma analysis of materials and boron neutron capture therapy for the eradication of inoperable tumors.

CONCLUSIONS

Extensive measurements of polycapillary performance and analysis of potential applications have been performed by a large number of researchers. Polycapillary optics appear to have a number of promising applications. The least demanding applications technically are those which require simple flux gains, such as diffraction, fluorescence, and other materials analysis applications. Applications which require monolithic optics are more difficult technically than those which rely on multifiber optics. The most demanding applications are imaging applications because a much smaller number of poor channels is tolerable. However, the technology for designing, producing, and measuring polycapillary optics is advancing quite rapidly.

ACKNOWLEDGMENTS

The author acknowledges the many collaborators whose work is excerpted in this paper, particularly the helpful discussions with Walter Gibson, who originated many of the concepts presented in this paper, and the pioneering work of Muradin Kumakhov. Numerical simulations, data, and discussions were provided by QiFan Xiao and David Gibson of X-Ray Optical Systems, Inc. Data and assistance were also provided by a large number of collaborators including Carmen Abreu, David Aloisi, Ray Benneson, David Bittel, Lee Britt, Ariel Caticha, Heather Chen, Greg Downing, Xiaoyang Fu, Ning Gao, Chris Jezewski, Kardiawarman, Andrei Karnaukhov, John Kimball, Ira Klotzko, David Kruger, Ed Manning, Devon Mason, David Mildner, Johanna Mitchell, Charles Mistretta, Wally Pepler, Sergei Poturaev, Igor Ponomarev, Bimal Rath, Johannes Ullrich, Michael Vartanian, Lei Wang, and Russel Youngman. This work was supported in part by ATP Award CA 70NANB2H1250, NSF Grant ISI-9160568, NIH Grants RO1 CA58521, 1 R43 CA58146, and 1 R43 HL49019, and by the NYS Center for Advanced Technology.

REFERENCES

1. F. JENTZCH, *Phys. Z.* **30**, 1268 (1929).
2. P. B. HIRSCH AND J. N. KELLER, *Phys. Soc. (London) Ser. B* **64** (1951).
3. V. A. ARKD'EV, A. I. KOLOMITSEV, M. A. KUMAKHOV, I. YU. PONORAVE, I. A. KHODEEV, YU. P. CHERTOV, AND I. M. SHAKPARONOV, *Sov. Phys. Usp.* **32**(3), 271 (Mar. 1989).
4. J. D. JACKSON, "Classical Electrodynamics," Wiley, New York, 1962.
5. C. A. MACDONALD, C. C. ABREU, S. BUDKOV, H. CHEN, X. FU, W. M. GIBSON, KARDIAWARMAN, A. KARNAUKHOV, B. KOVANTSEV, I. PONOMAREV, B. K. RATH, J. B. ULLRICH, M. VARTANIAN, AND Q. F. XIAO, in "Multilayer and Grazing Incidence X-Ray/EUV Optics II" (R. B. Hoover and A. Walker, Eds.), SPIE Procs., Vol. 2011, SPIE 1993.
6. J. B. ULLRICH, V. KOVANTSEV, AND C. A. MACDONALD, *J. Appl. Phys.* **74**(10), (Nov. 15, 1993).
7. S. POTARIEV AND Q. F. XIAO, personal communication.
8. B. K. RATH, R. YOUNGMAN, AND C. A. MACDONALD, "An Automated Test System for Measuring X-Ray Transmission through Polycapillaries," *Rev. Sci. Instrum.* **65**, 3393 (Nov. 1994).
9. Q. F. XIAO, I. Y. PONAMAREV, A. I. KOLOMITSEV, AND J. C. KIMBALL, in "X-Ray Detector Physics and Applications" (R. B. Hoover, Ed.), SPIE, 1992.
10. B. L. HENKE, E. M. GULLIKSON, AND J. C. DAVIS, *At. Data Nucl. Data Tables* **54**(2), 181, (1993).
11. D. BITTEL AND J. KIMBALL, Theoretical effects of surface roughness on capillary optics, *J. Appl. Phys.* **74**(2), (1993).
12. V. E. KOVANTSEV, J. PANT, V. PANTOJAS, N. NAZARYAN, T. M. HAYES, AND P. D. PERSANS, *Appl. Phys. Lett.* **62**(23), 2906 (1993).
13. KARDIAWARMAN, V. KOVANTSEV, S. BUDKOV, Q. F. XIAO, W. M. GIBSON, T. M. HAYES, L. LURIO,

- C. A. MACDONALD, P. D. PERSANS, AND Q. F. XIAO, "Characterization of a Multi-Fiber Polycapillary-Based X-Ray Collimating Lens," SPIE Proceedings 1994, SPIE,
14. J. B. ULLRICH, I. YU. PONOMAREV, M. V. GUBAREV, N. GAO, Q.-F. XIAO, AND W. M. GIBSON, "Development of Monolithic Capillary Optics for X-Ray Diffraction Applications," SPIE Proceedings 1994.
 15. M. VARTANIAN, R. YOUNGMAN, D. GIBSON, J. DRUMHELLER, AND R. FRANKEL, "Polycapillary Collimator for Point Source Proximity X-Ray Lithography," *J. Vac. Sci. Technol. B* **11**(6), (Nov/Dec 1993).
 16. J. B. ULLRICH, W. M. GIBSON, M. V. GUBAREV, AND C. A. MACDONALD, *Nucl. Instrum. and Methods A* **347**, 401 (1994).
 17. W. M. GIBSON AND M. A. KUMAKHOV, in "Yearbook of Science & Technology," p. 488–490, McGraw–Hill, New York, 1993.
 18. P. A. TOMKINS, C. C. ABREU, F. E. CARROLL, Q. F. XIAO, AND C. A. MACDONALD, "Use of Capillary Optics as a Beam Intensifier for a Compton X-Ray Source," *Med. Phys.* **21** (11), 1777 (1994).
 19. W. M. GIBSON AND M. A. KUMAKHOV, in "X-Ray Detector Physics and Applications," p. 172, SPIE Vol. 1736, SPIE 1992.
 20. A. I. KHODEEV, S. I. KHODEEV, AND I. YU. PONOMAREV, "Transformation of the X-Ray Image with the Capillary System," personal communication.
 21. D. G. KRUGER, C. C. ABREU, W. W. PEPLER, C. A. MACDONALD, AND C. A. MISTRETTA, "Imaging Characteristics of X-Ray Capillary Optics in Mammography," *Medical Physics*, in press.
 22. C. C. ABREU, D. G. KRUGER, C. A. MACDONALD, C. A. MISTRETTA, W. W. PEPLER, AND Q. F. XIAO, "Measurements of Capillary X-Ray Optics with Potential for use in Mammographic Imaging," *Med. Phys.*, in press.
 23. H. L. MANNING, R. E. SHEFER, R. E. KLINKOWSTEIN, AND C. A. MISTRETTA, *Med. Phys.* **18**, 880 (1991).
 24. H. CHEN, R. G. DOWNING, D. F. R. MILDNER, W. M. GIBSON, M. A. KUMAKHOV, I. YU. PONOMAREV, AND M. V. GUBAREV, *Nature*, **357**, 391 (1992).